© 2017. Published by The Company of Biologists Ltd | Journal of Experimental Biology (2017) 220, 3649-3656 doi:10.1242/jeb.153494

RESEARCH ARTICLE

# Asymmetry costs: effects of wing damage on hovering flight performance in the hawkmoth *Manduca sexta*

**María José Fernández*, Marion E. Driver and Tyson L. Hedrick‡**

## ABSTRACT

Flight performance is fundamental to the fitness of flying organisms. Whilst airborne, flying organisms face unavoidable wing wear and wing area loss. Many studies have tried to quantify the consequences of wing area loss to flight performance with varied results, suggesting that not all types of damage are equal and different species may have different means to compensate for some forms of wing damage with little to no cost. Here, we investigated the cost of control during hovering flight with damaged wings, specifically wings with asymmetric and symmetric reductions in area, by measuring maximum load lifting capacity and the metabolic power of hovering flight in hawkmoths (*Manduca sexta*). We found that while asymmetric and symmetric reductions are both costly in terms of maximum load lifting and hovering efficiency, asymmetric reductions are approximately twice as costly in terms of wing area lost. The moths also did not modulate flapping frequency and amplitude as predicted by a hovering flight model, suggesting that the ability to do so, possibly tied to asynchronous versus synchronous flight muscles, underlies the varied responses found in different wing clipping experiments.

**KEY WORDS: Flight control, Metabolism, Stability, Wing wear, Respirometry**

## INTRODUCTION

Flying organisms face unavoidable wing wear and wing area loss due to collisions with the environment, competition and even predation. Losing wing area may have negative consequences for an organism's flight performance; these negative consequences may be exacerbated by bilateral asymmetries in the area loss. Here, we investigated the costs to maximum load lifting capacity and flight efficiency (here, overall lift to power ratio) brought about by asymmetric and symmetric wing damage.

Asymmetric wing damage results in a stability challenge as well as a reduction in aerodynamic efficiency and maximum lift force because if the wings are asymmetric, symmetric wing kinematics no longer produce symmetric forces and torques. Therefore, the animal must use asymmetric wing kinematics to produce symmetric forces and torques, potentially increasing the difficulty and cost of compensating for the wing damage. Nevertheless, animals with asymmetric wing damage are able to maintain flight stability and perform complex manoeuvres (Haas and Cartar, 2008), suggesting that insects may possess capabilities for reducing the costs of wing asymmetry.

Animals are able to maintain stability when perturbed using active neural mechanisms, passive non-neural mechanisms or a combination of the two (Dickinson et al., 2000; Nishikawa et al., 2007). For example, studies of flapping flight show that organisms are able to overcome some types of perturbation with minimal neural input through the intrinsic stabilizing effects of flapping (Hedrick et al., 2009; Ristroph et al., 2010). But, organisms also use active neural modulation to perform voluntary manoeuvres, like yaw turns in aerial locomotion (Springthorpe et al., 2012). Moreover, Fernández et al. (2012) showed that hawkmoths with asymmetric wings control and maintain stability during hovering through neural modulation of muscle activity once the amount of wing area loss exceeds ∼10%. In this case, the moths have to constantly steer to counteract the torque produced by the wing asymmetry. The constant manoeuvring required of the neuromuscular system with asymmetric wings may be costly to other aspects of flight performance such as maximum lift production, where some aerodynamic force will be assigned to flight control rather than weight support. Furthermore, it will affect the animal's metabolic power requirement, as some additional flight force beyond that required to support the body must be generated and devoted to steering.

Many studies have tried to quantify the consequences to flight performance of wing area loss. However, they have produced disparate results, indicating that not all types of damage are equal and that different species may have different means to compensate for some forms of wing damage with little to no cost. For example, a study of metabolic power expenditure in hovering hummingbirds found no costs associated with natural reductions in wing area during moulting (Chai, 1997). Similarly, Hedenström et al. (2001) showed no increase in metabolic power when artificially reducing wing area in bumblebees. The same outcome has also been found in bats with naturally asymmetric wings (Voigt, 2013), and birds were found to suffer more from symmetric than from asymmetric damage of similar total magnitude (Hambly et al., 2004). Furthermore, studies of insects have found that individuals with reduced wing area have fitness similar to that of individuals without damaged wings (e.g. butterflies: Kingsolver, 1999; and bumblebees: Haas and Cartar, 2008). However, other studies have shown decreases in various measures of flight performance following natural and artificial wing damage in birds (Swaddle, 1997) and insects (Combes et al., 2010; Vance and Roberts, 2014; Mountcastle et al., 2016).

Here, we study the cost of hovering flight with damaged wings, specifically wings with asymmetric and symmetric reductions in area. We investigate the cost of control during hovering flight with asymmetric wings by measuring maximum load lifting capabilities and the metabolic power of flight through respirometry (oxygen consumption and carbon dioxide production) in hawkmoths (*Manduca sexta*).

Department of Biology, University of North Carolina, Chapel Hill, NC 27599, USA. *Present address: Department of Life Sciences, University of Roehampton, London SW15 4JD, UK.

‡Author for correspondence (thedrick@bio.unc.edu)

T.L.H., 0000-0002-6573-9602

**Received 18 November 2016; Accepted 4 August 2017**

Journal of Experimental Biology (2017) 220, 3649-3656 doi:10.1242/jeb.153494

Classic flapping flight aerodynamic models provide a predictive framework for examining the effects of wing area loss on flight performance using the second and third moments of wing area, which weigh the aerodynamic importance of wing area by its distance from the wing root or base (Ellington, 1984b; Weis-Fogh, 1973). From these models, we hypothesized that the maximum load lifted by the moth decreases proportional to the cube root of the fractional change in second moment of wing area, while the metabolic cost of hovering flight increases in proportion to the decrease in the lift to power ratio; the hypothesized increase in cost is in proportion to the reduction in the third moment of wing area raised to the −0.5 power. Alternatively, if the moths are not able to adjust their flapping frequency or amplitude, maximum load lifted is predicted to decline in linear proportion to the decrease in the second moment of wing area. In all cases, we predicted that asymmetric wing damage will lead to reduced performance compared with symmetric damage of similar magnitude, as has been found previously in flying birds (Balmford et al., 1993; Swaddle, 1997). For equations and more details about the models, see 'Aerodynamic model' section in Materials and methods.

## MATERIALS AND METHODS

### Animals and experimental design

We obtained male *Manduca sexta* (Linnaeus 1763) pupae from the Department of Biology at Duke University. After eclosion, adult moths were housed in mesh fabric cages (30×30×30 cm) at 25±3°C under a 22 h:2 h light:dark photoperiod to minimize activity and avoid unintended wing damage. We trained moths, on the third day following eclosion, by presenting them with a natural and artificial flower to stimulate their feeding behaviour and therefore elicit stable hovering flight. Moths were chosen as experimental candidates after demonstrating prolonged and stable hovering flight in front of the flower. We measured asymptotic load lifting and respirometry (oxygen consumption and carbon dioxide production; see below for details) in moths exposed to three experimental conditions (Fig. 1): (i) fully intact wings (unclipped), (ii) asymmetric wing clipping (one forewing clipped; side randomly chosen) and (iii) approximately symmetric wing clipping (the two forewings similarly clipped). To perform all treatments in each individual, we applied the treatments in order, randomly varying which wing received the damage in the asymmetric treatment. We clipped each individual forewing tip, from the trailing edge to the leading edge, with scissors (Fig. 1), resulting in a total wing area reduction of between 7% and 24%. These area reductions are similar in magnitude to those found in nature in wild bumblebees (Cartar, 1992). Wing clipping typically caused the moths to attempt to seek shelter and not respond to the food and flower stimulus used to elicit flight behaviour. Thus, moths were given 12–24 h to recover from clipping before they were used in the next assay. Moths were housed in the aforementioned mesh cages and given access to water *ad libitum* during this time.

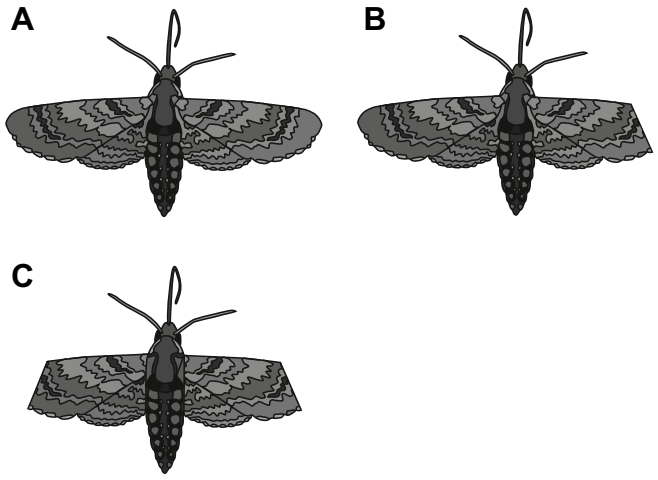


**Fig. 1. Schematic representation of the treatments applied to each individual moth during asymptotic load-lifting and respirometry measurements.** (A) Control or fully intact wings. (B) Asymmetric wing clipping, where the moth has only one forewing tip clipped. (C) Symmetric wing clipping, where both forewings have been clipped.

### Asymptotic load lifting

We performed asymptotic load lifting to quantify maximum vertical aerodynamic force production (Buchwald and Dudley, 2010; Chai et al., 1997; Dillon and Dudley, 2004). Briefly, we attached a rubber band with a 2 cm loop of string near the moth's centre of body mass (between the thorax and abdomen). A beaded string with 7–9 beads at 2 cm intervals (0.2±0.0001 g each; Adventurer Pro, Ohaus Corporation, Parsippany, NJ, USA) was then attached 3 cm below the loop. We placed the trained moth in the bottom of a flight chamber (0.7×0.7×0.7 $m^3$) illuminated with eight infrared lights (760 nm; Roithner LaserTechnik GmBH, Vienna, Austria). After the individuals were placed in the bottom of the chamber, they began to fly upwards, progressively lifting more beads off the ground until reaching their load-carrying capacity. To encourage the moths to fly vertically and hover stably with a maximum load, we used a flower stimulus. Load-lifting trials were recorded with high-speed video and typically lasted less than 10 s. We discarded recordings where the individual did not fly vertically or its proboscis contacted the flower.

Each individual was exposed to the three experimental treatments (described above): unclipped, asymmetric wing clipping and symmetric wing clipping. During the load-lifting trials, we removed 7–23% of the area of a single wing, which corresponded to a 17–49% decrease in the second moment of area, when clipping the wings for the asymmetric clipping treatment (see Table S1).

We calculated maximum load by adding the mass of all beads lifted and the moth mass. After each treatment, we measured the individual's body mass. Maximum vertical force ($F_{V,max}$) was then calculated as the product of the maximum load and gravitational acceleration. During load lifting, flight kinematics were recorded at 1000 Hz using three orthogonally positioned high-speed cameras (two Phantom v7.1 and one Phantom v5.1; Vision Research, Wayne, NJ, USA). From the videos, we extracted wing stroke amplitude (θ) and wingbeat frequency (η) for each treatment through a 3D kinematic reconstruction (DLTdv5; Hedrick, 2008; see Table S2).

After the last treatment, individuals were frozen for wing preservation. Clipped forewings and their fragments were later placed together and scanned for morphological measurements (see Table S1). We investigated the effect of symmetric and asymmetric wing damage (as fixed effects) on maximum vertical aerodynamic force production ($F_{V,max}$) and wing kinematics (η and θ) using a linear mixed-effects model (nlme package, R3.3.1; Pinheiro and Bates, 2000; http://CRAN.R-project.org/package=nlme; https://www.R-project.org/) with random intercepts for each individual (Pinheiro and Bates, 2000).

We also categorized the magnitude of the wing clipping to further examine the effect of wing area loss on maximum vertical force. A 'small' area was <12% of wing area, which is similar to what is

Journal of Experimental Biology (2017) 220, 3649-3656 doi:10.1242/jeb.153494

found in nature in wild bumblebees (Cartar, 1992), while a 'large' area was >12% (maximum of 23%); around an 18% decrease in wing area is the upper extreme of wear normally found in nature (Cartar, 1992). We chose these magnitudes as it has been shown that individuals with ≤10% wing area loss are more likely to use a passive mechanism to maintain flight stability, while individuals with >10% wing damage are more likely to use an active mechanism, suggesting a more costly flight performance (Fernández et al., 2012); we used the 12% dividing line to split our dataset in half near this previously supported point. To investigate the magnitude of the clipping, we used a subset of the data (asymmetric and symmetric clipping only) in a linear mixed-effects model (nlme package, R3.3.1; Pinheiro and Bates, 2000; http://CRAN.R-project.org/package=nlme; https://www.R-project.org/) of the relationship between maximum vertical aerodynamic force production and clipping treatment.

### Respirometry

We determined moth metabolic rate during the above-mentioned three experimental treatments to quantify the cost of hovering with asymmetric and symmetric wings. The measured volume of $O_2$ consumption and $CO_2$ production was divided by the time the moth spent hovering in a sealed Plexiglas chamber (9.4 l) to obtain the individual's metabolic rate (see Table S3). Measurements were done at room temperature (23±2°C).

Immediately following a warm-up flight, moths were placed in a cylindrical enclosure, 20 cm in diameter and 30 cm in height (Fig. 2A). Moths flew for between 3 and 12 min, measured with a chronometer. Once the moth stopped flying, we took a 50 ml sample of air from the flight chamber with a large syringe (60 ml). We injected the gas sample through a three-way valve to a Foxbox oxygen and carbon dioxide analyser (Sable Systems International, Las Vegas, NV, USA), passing through a column of desiccant (Drierite, Xenia, OH, USA) for the removal of water vapour. This method allowed us to measure $CO_2$ production ($\dot{V}_{CO_2}$) and $O_2$ consumption ($\dot{V}_{O_2}$) in moths, therefore enabling us to calculate the respiratory quotient, RQ (i.e. the ratio of $\dot{V}_{CO_2}$ to $\dot{V}_{O_2}$), and ascertain the fuel that the moths were using. As such, our methodology was preferable to the more conventional flow-through respirometry approach, which, with the equipment available here, would not have permitted $O_2$ measurement in the large flight volume.

During the analysis, we only considered trials that lasted more than 2 min with the moth flying continuously in the centre of the chamber. For calculation of the flight efficiency among treatments, we used the ratio between the predicted mechanical power, using Eqns 1, 2 and 5, and the metabolic power calculated from the raw $O_2$ consumption data (see 'Aerodynamic model', below, for equations).

After the last treatment, as for individuals used during the asymptotic load lifting, individuals were frozen for wing preservation and clipped forewings were later reconstructed and scanned for morphological measurements (see Table S1). Note that the set of individuals used for the respirometry experiments ($n$=6) differs from the set used for load lifting ($n$=8) and that the respirometry rig and recording duration precluded the use of high-speed video to measure wing kinematics.

We investigated the effect of treatment (symmetric and asymmetric wing clipping), as fixed effects, on metabolic power, $\dot{V}_{O_2}$ consumption, $\dot{V}_{CO_2}$ production and RQ using a linear mixed-effects model (nlme package, R3.3.1; Pinheiro and Bates, 2000; http://CRAN.R-project.org/package=nlme; https://www.R-project.org/) with random intercepts for each individual (Pinheiro and Bates, 2000).

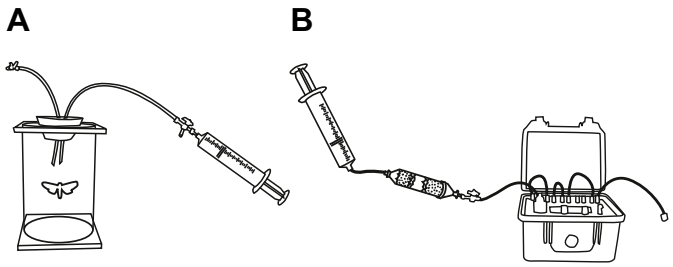


**Fig. 2. Experimental apparatus.** Schematic representation of the hovering flight chamber (A) and the portable oxygen and carbon dioxide analyser (B).

### Aerodynamic model

Following Ellington (1984b), the lift from a flapping wing with zero forward velocity, i.e. when hovering, may be modelled as:

$$L = \frac{1}{8}\rho S_2 n^2 \phi^2 \overline{C_l}\,\overline{(\mathrm{d}\hat{\phi}/\mathrm{d}\hat{t})^2}, \quad (1)$$

where ρ is air density, $S_2$ is the second moment of wing area, $n$ is the flapping frequency, $\phi$ is the flapping amplitude, $\overline{C_l}$ is the average coefficient of lift and $\overline{(\mathrm{d}\hat{\phi}/\mathrm{d}\hat{t})^2}$ is the average square of the non-dimensional angular velocity. The mechanical power required for flapping is given by:

$$P_{\mathrm{mech}} = \frac{1}{16}\rho S_3 n^3 \phi^3 \overline{C_d}\,\overline{|\mathrm{d}\hat{\phi}/\mathrm{d}\hat{t}|^3}, \quad (2)$$

where $S_3$ is the third moment of wing area, $\overline{C_d}$ is the average coefficient of drag and $\overline{|\mathrm{d}\hat{\phi}/\mathrm{d}\hat{t}|^3}$ is the average of the absolute value of the cube of the non-dimensional angular velocity of flapping. A reduction in wing area will also reduce the second and third moments of wing area. Thus, if all other parameters remain unchanged, a moth with reduced wing area will produce less lift and require less muscle power to flap its wings. In this case, the lift following clipping, $L'$, is given by:

$$L' = L\left(\frac{S'_2}{S_2}\right), \quad (3)$$

where $S'_2$ is the second moment of wing area following clipping. Note that in this case, the power required to flap the wings also decreases even though clipping the wing tip is not expected to reduce the available muscle power. If the moth were to increase its flapping amplitude or frequency such that power output before and after clipping were identical, lift following clipping, $L'$, would be equal to:

$$L' = L\left(\frac{S'_2}{S_2}\right)\left(\frac{S'_3}{S_3}\right)^{-2/3}, \quad (4)$$

where $S'_3$ is the third moment of wing area following clipping. This equation allows prediction of the effect of clipping on maximum load lifted, assuming that load lifted is limited by muscle power before and after clipping.

An increase in flapping frequency or amplitude increases both lift (Eqn 1) and mechanical power (Eqn 2) but alters their ratio; increases in frequency or amplitude decrease efficiency (i.e. lift to power ratio). This forms the basis for a prediction of the effect of wing clipping on the energetic cost of hovering flight. If $L'$ is to be maintained at its original value as in a hovering moth supporting its own weight, then $P'_{\mathrm{mech}}$, the mechanical power of hovering following wing clipping and compensation by changing flapping

Journal of Experimental Biology (2017) 220, 3649-3656 doi:10.1242/jeb.153494

frequency or amplitude, is given by:

$$P'_{\text{mech}} = P_{\text{mech}} \frac{S'_3}{S_3} \left(\frac{S'_2}{S_2}\right)^{-3/2}. \quad (5)$$

If the fractional reductions in the second and third moment of wing area are assumed to be equal, and they are often similar in practice, then Eqns 4 and 5 reduce to:

$$L' \cong L\left(\frac{S'_2}{S_2}\right)^{1/3}, \quad (6)$$

$$P'_{\text{mech}} \cong P_{\text{mech}}\left(\frac{S'_3}{S_3}\right)^{-1/2}. \quad (7)$$

To estimate the mechanical power required for hovering under the three experimental conditions, we solved Eqn 1 for the flapping frequency η required to support body weight, assuming ϕ of 115 deg, ρ of 1.22 kg m$^{-3}$, $\overline{C_l}$ of 1.4 and $\overline{(\mathrm{d}\hat{\phi}/\mathrm{d}\hat{t})^2}$ of 19.74 characteristic of sinusoidal motion (Ellington, 1984a; see Appendix), then used the resulting η with Eqn 2 to estimate power, with $\overline{C_d}$ of 1.6 and $\overline{|\mathrm{d}\hat{\phi}/\mathrm{d}\hat{t}|^3}$ of 105.29 (i.e. sinusoidal flapping; see Appendix). These results were then adjusted for clipping using Eqn 5. Note that other compensatory mechanisms exist such as changes in $\overline{C_l}$ and none of the aerodynamic models can accommodate the effect of wing asymmetry. In calculating the expected $L'$ and $P'_{\text{mech}}$ for asymmetric moths, we used the total wing area and moments, summing the clipped and unclipped wings. Thus, if asymmetry itself has a cost, the models would tend to underestimate the effect of asymmetric area loss on performance. For these reasons, we expect the models to furnish no more than a general prediction of effect magnitude and direction rather than exact predictions of changes in maximum load or flight efficiency.

The above equations do not include any costs for the inertial power requirements of flapping because the degree to which these costs are additive with aerodynamic costs and not recovered elastically or by conversion to aerodynamic forces is unknown. Current models of flight power commonly bracket the possible range of outputs by considering cases with 0% and 100% of inertial costs included in the final result, e.g. Cheng et al. (2016). However, comparison of recent detailed computational fluid simulations of hawkmoth flight with costs measured by respirometry suggest that hawkmoths are probably closer to the 0% than to the 100% case (Zheng et al., 2013). Thus, we do not include inertial costs in the above analysis but do discuss them below.

Following work by Ellington (1984b), the inertial cost of flapping is given by:

$$P_{\text{inertial}} = 2nm_2(\mathrm{d}\phi/\mathrm{d}t)^2_{\text{max}}, \quad (8)$$

where $m_2$ is the second moment of wing mass and is proportional to the second moment of wing area for a wing of constant density and thickness. The inertial power required for the virtual mass, i.e. fluid accelerated with the wing, is also proportional to the second moment of area. In both the actual and virtual mass cases, if flapping frequency is increased to maintain lift following wing damage, the inertial power requirement as a whole increases such that:

$$P'_{\text{inertial}} \cong P_{\text{inertial}}\left(\frac{S'_2}{S_2}\right)^{-1/2}, \quad (9)$$

assuming that the wing is of constant thickness and density in the actual mass case. Real hawkmoth wings are thicker toward the root by a degree difficult to include in analytic expressions such as Eqn 9 and this tendency will make $P'_{\text{inertial}}$ due to actual mass greater than predicted by Eqn 9. However, in general, this analysis suggests that for the flight efficiency case, inertial power and aerodynamic power vary similarly.

This is also true for the case where flapping frequency is increased to restore mechanical power output following clipping. Here, $P'_{\text{inertial}} \cong P_{\text{inertial}}$ given the aforementioned assumption of constant thickness and density as well as the assumption of equal reduction in the second and third moment of wing area as was used in Eqns 6 and 7. Thus, at the level of detail we believe simple models such as these capture, our model and predictions are not influenced by whether or not inertial power is included in the metabolic or muscle costs.

## RESULTS

### Asymptotic load lifting

Overall mean±s.e.m. values for maximum vertical aerodynamic force production ($F_{\text{V,max}}$) and wingbeat kinematics (η and θ) are given in Table 1 for each experimental treatment and also in Table 2, separated by small and large area clipped.

As expected, wingbeat frequency (η) increased following wing clipping. The linear mixed-effects model with random effects based on individual moths showed that wingbeat frequency was significantly different between the unclipped and symmetric clipping treatments (lme, $P$=0.036, $n$=8; Table 3). However, the unclipped and asymmetric treatments did not differ, nor was the asymmetric treatment different from the symmetric wing clipping (lme, $P$=0.15 and $P$=0.42 respectively, $n$=8; Table 3).

In the case of wing stroke amplitude (θ), the linear mixed-effects model showed that the asymmetric treatment was significantly different from the symmetric clipping treatment (lme, $P$=0.02; Table 3). The model also showed a marginally significant difference between the unclipped and the symmetric wing clipping treatments (lme, $P$=0.05, $n$=8; Table 3). However, we found no significant difference between the asymmetric and unclipped treatments (lme, $P$=0.64, $n$=8; Table 3).

As expected, the reduction in wing second moment of area was associated with a decrease in maximum vertical aerodynamic force production ($F_{\text{V,max}}$). We found that $F_{\text{V,max}}$ decreased significantly between the unclipped and clipped treatments (lme, $P$<0.001, $n$=8; Tables 1 and 3, Fig. 3). However, $F_{\text{V,max}}$ following asymmetric clipping was not significantly different from that for the symmetric treatment (lme, $P$=0.40, $n$=8; Table 3).

We also found that $F_{\text{V,max}}$ decreased more than expected as per Eqn 3 when clipping wings asymmetrically [lme, $\Delta F_{\text{V,max}}$=1.32×$\Delta S_2$ (the percent reduction in second moment of area), $r^2$=0.56; Fig. 3]. In contrast, clipping wings symmetrically

**Table 1. Maximum vertical aerodynamic force production ($F_{\text{V,max}}$) and wingbeat kinematics (η and θ) during treatments**

| | Unclipped | Asymmetric wings | Symmetric wings |
|---|---|---|---|
| $F_{\text{V,max}}$ (N) | 0.0256±0.001 | 0.0212±0.001 | 0.0203±0.001 |
| η (Hz) | 28.78±0.492 | 29.38±0.521 | 29.71±0.195 |
| θ (deg) | 116.98±2.105 | 115.85±1.629 | 121.99±1.490 |
| $\theta_{\text{l–r}}$ (deg) | 6.31±1.898 | 15.29±6.031 | 5.71±1.563 |

η, wingbeat frequency; θ, stroke amplitude; $\theta_{\text{l–r}}$, stroke amplitude difference between the left and right wings.
Values were generated using all individuals ($n$=8). Data are means±s.e.m.
Data used for this table are available in Table S1.



Journal of Experimental Biology

Journal of Experimental Biology (2017) 220, 3649-3656 doi:10.1242/jeb.153494

**Table 2. Load-lifting data according to small (S) and large (L) area clipping group during each experimental treatment**

| | $F_{V,max}$ (N) | | η (Hz) | | θ (deg) | | | |
|---|---|---|---|---|---|---|---|---|
| | | | | | S | | L | |
| | S | L | S | L | Left | Right | Left | Right |
| Unclipped | 0.027±0.0013 | 0.024±0.0013 | 28.21±0.44 | 29.34±0.78 | 117.71±2.32 | 120.78±3.20 | 111.62±2.73 | 118.94±4.37 |
| Asymmetric wings | 0.025±0.0005 | 0.017±0.0007 | 28.44±0.23 | 30.19±0.70 | 118.52±4.10* | 116.05±3.13 | 127.16±2.69* | 102.40±5.01 |
| Symmetric wings | 0.024±0.0006 | 0.017±0.0012 | 29.45±0.31 | 30.08±0.32 | 122.75±4.98 | 117.71±1.28 | 125.08±2.75 | 121.57±0.81 |

$F_{V,max}$, maximum vertical aerodynamic force; η, wingbeat frequency; θ, wingbeat amplitude for both wings (left and right). *Data from the clipped wing. Values were generated using all individuals ($n$=8, $n$=4 each in S and L). Data are means±s.e.m.

resulted in a decrease in $F_{V,max}$, but had a smaller effect than asymmetric clipping, as indicated by the differences in the $F_{V,max}$/second moment of area slope for the two treatments (lme, $F_{V,max}$=0.78×Δsecond moment of area, $r^2$=0.77). In addition, the interaction between the two factors treatment and Δsecond moment of area was significant (lme, $P$=0.02, $n$=8; Fig. 3). To further examine the effect of wing area loss on maximum vertical force, we categorized the magnitude of wing clipping. We found a significant reduction in $F_{V,max}$ depending on clipping magnitude. When clipping a larger area of the wing, we found a significant decrease in force in the asymmetric treatment compared with the unclipped treatment (lme, $P$=0.0001, $n$=4; Table 2, Fig. 4) – indeed, a further decrease from what was expected from the aerodynamic model ($F_{V,max}$∝second moment of area; Eqn 4). The symmetric treatment also produced a significant decrease in $F_{V,max}$ (lme, $P$=0.0001, $n$=4), but there was no significant difference between the asymmetric and symmetric treatments for the large clipping group (lme, $P$=0.49, $n$=4). In comparison, when we clipped only a small percentage of the wing, we found an approximately linear reduction of $F_{V,max}$ in the asymmetric treatment (lme, $P$=0.13, $n$=4) and a significant further decrease in force when clipping wings symmetrically compared with the unclipped treatment (lme, $P$=0.02, $n$=4; Fig. 4). Similar to the magnitude of the effect of the large clipping treatment, we did not find a significant difference between the asymmetric and symmetric treatments (lme, $P$=0.30, $n$=4; Table 2).

### Respirometry and flight efficiency

Overall mean±s.e.m. values for metabolic power ($P_{met}$), mass-specific carbon dioxide production ($\dot{V}_{CO_2}$), mass-specific oxygen consumption ($\dot{V}_{O_2}$), RQ and the predicted mechanical power ($P_{mech}$) are given in Table 4 for each experimental treatment.

**Table 3. Linear mixed-effects model showing the effect of treatment on maximum vertical aerodynamic force ($F_{V,max}$) and wingbeat kinematics (η and θ)**

| Variable | $t$-value | $P$-value |
|---|---|---|
| $F_{V,max}$ | | |
| Unclipped vs asymmetric | 4.432 | 0.0006 |
| Unclipped vs symmetric | 5.303 | 0.0001 |
| Asymmetric vs symmetric | 0.871 | 0.398 |
| η | | |
| Unclipped vs asymmetric | 1.528 | 0.152 |
| Unclipped vs symmetric | 2.353 | 0.036 |
| Asymmetric vs symmetric | 0.825 | 0.425 |
| θ | | |
| Unclipped vs asymmetric | 0.485 | 0.636 |
| Unclipped vs symmetric | 2.164 | 0.051 |
| Asymmetric vs symmetric | 2.649 | 0.021 |

η, wingbeat frequency; θ, wingbeat amplitude.
Individuals were used as a random effect ($n$=8 moths). Data used for this table are available in Table S1.

$P_{met}$ was affected by the asymmetric and symmetric treatments: clipped moths exhibited greater $P_{met}$ compared with moths with unclipped wings. The linear mixed-effects model showed a significant difference between the unclipped and the clipped treatments (lme, $P$=0.005; $n$=6; Table 5, Fig. 5). However, there was no significant difference between asymmetric and symmetric treatments (lme, $P$=0.98; $n$=6; Table 5, Fig. 5).

Mass-specific $\dot{V}_{O_2}$ and $\dot{V}_{CO_2}$ increased with clipping treatments. When looking at mass-specific $\dot{V}_{O_2}$, the linear mixed-effects model showed a significant difference between the unclipped and clipped treatments (lme, $P$=0.008 for asymmetric treatment and $P$=0.007 for symmetric treatment; $n$=6; Table 5) but no significant difference between the two clipping treatments (lme, $P$=0.93; $n$=6; Table 5). Identical patterns of significance were found for mass-specific $\dot{V}_{CO_2}$ (lme, $P$<0.001 between unclipped and asymmetric treatments; $P$=0.002 between unclipped and symmetric treatments; and $P$=0.42 between clipping treatments; $n$=6; Table 5).

The ratio of $\dot{V}_{CO_2}$ to $\dot{V}_{O_2}$ varied among moths and there was a trend toward higher RQ values in the clipped-wing moths. The linear mixed-effects model showed a significant difference between the unclipped and asymmetric clipping treatment (lme, $P$=0.022; $n$=6; Table 5) but no significant difference between unclipped and symmetric clipping (lme, $P$=0.414; $n$=6) and between clipping treatments (lme, $P$=0.094; $n$=6; Table 5). The average (±s.e.m.) RQ among all moths and treatments was 0.84±0.017 (Table 4).

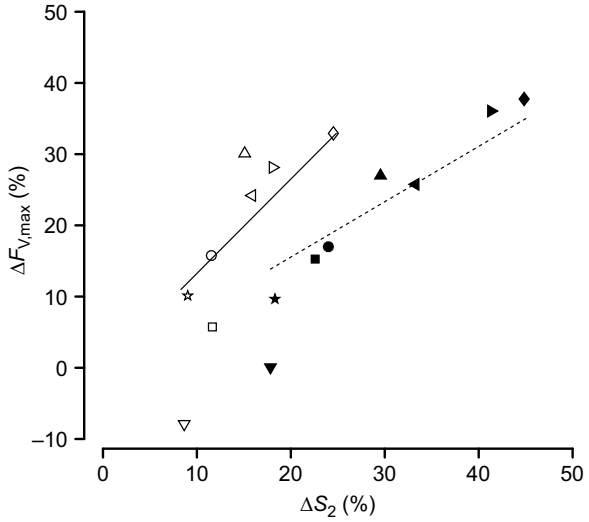


**Fig. 3. Effect of clipping treatment on maximum vertical force produced by eight moths.** Reduction in maximum vertical force ($F_{V,max}$) is plotted against the reduction in the second moment of wing area ($S_2$). Moths are individually indicated by marker shape (asymmetric clipping, filled markers; symmetric clipping, open markers). A linear fit to the data for each treatment is shown: symmetric clipping, slope 0.78 ($r^2$=0.77, $P$=8.31×10$^{-7}$); asymmetric clipping, slope 1.32 ($r^2$=0.56, $P$=5.23×10$^{-6}$).

Journal of Experimental Biology (2017) 220, 3649-3656 doi:10.1242/jeb.153494

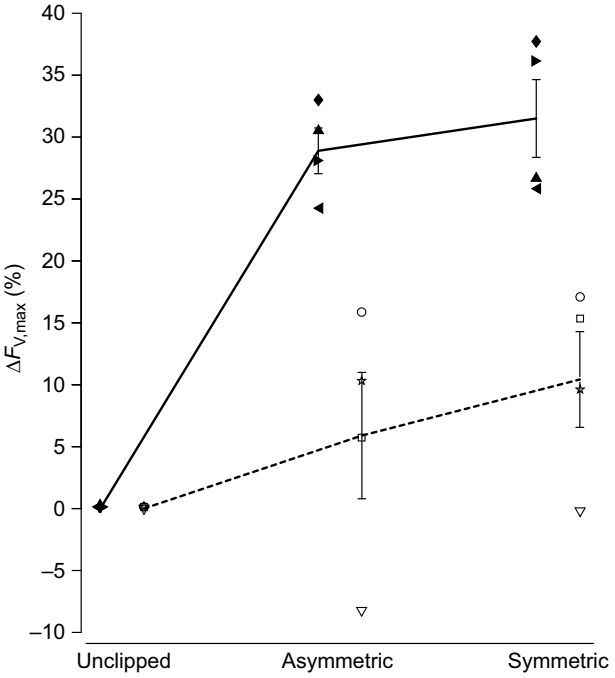


**Fig. 4. Effect of experimental treatment (unclipped, asymmetric and symmetric) on the percentage decrease in maximum vertical aerodynamic force ($F_{V,max}$).** Filled markers represent a large area clipped (12–23%) and open markers represent a small area clipped (7–10%). Marker shape corresponds to that in Fig. 3. Data are means±s.e.m.

Mechanical power ($P_{mech}$) was estimated using Eqns 1, 2 and 5 to look at the effects of wing clipping on efficiency (in this case, the ratio between the estimated mechanical power and the measured metabolic power). We found that estimated $P_{mech}$ increased with wing clipping (Table 4). The linear mixed-effects model showed a significant difference between the unclipped and both clipping treatments (lme, $P$=0.003 for asymmetric and $P$<0.001 for symmetric treatment; $n$=6; Table 5) and also between moths with asymmetrically and symmetrically clipped wings (lme, $P$=0.006; $n$=6; Table 5). Note that this $P_{mech}$ estimate from our simplified aerodynamic model does not indicate that $P_{mech}$ actually varied in the way described; the model cannot estimate any additional costs due to asymmetry. Instead, it shows that the three treatments (unclipped, asymmetric clip and symmetric clip) produce enough variation in expected power requirements that they should be distinguishable even given the small sample size, variation in morphology and variation in clipping treatment magnitude. Finally, the model operates by computing a flapping frequency for each specific moth from the morphological data and aerodynamic assumptions; these were 26.4±1.4, 28.2±2.5 and 31.1±1.4 Hz (mean±s.d., $n$=6) for the unclipped, asymmetric and symmetric treatments, respectively.

When we looked at the effects of wing clipping on efficiency, we found, as expected, that efficiency decreased with clipping treatment, being lowest in the asymmetric treatment. The linear mixed-effects model showed a significant difference between the unclipped and asymmetric treatments (lme, $P$=0.02; $n$=6; Table 5) but no significant difference between the unclipped and symmetric treatments (lme, $P$=0.24; $n$=6; Table 5) or between clipping treatments (lme, $P$=0.16; $n$=6; Table 5). The absence of a significant difference in efficiency between unclipped and symmetric treatments was surprising as the components of efficiency, $P_{mech}$ and $P_{met}$, do exhibit a significant difference. The result appears to be due to the decline in signal to noise ratio brought about by the combination of the two results.

## DISCUSSION

### Costs of damage and asymmetry

Our investigation of the costs of asymmetric and symmetric wing damage to the maximum load-lifting performance and metabolic cost of hovering flight in hawkmoths demonstrated substantial and significant negative effects of wing damage, especially asymmetric damage, in the hawkmoth *M. sexta*. To a first approximation, the effect of asymmetric damage was twice that of symmetric damage on a per-area basis, demonstrating a substantial additional cost of asymmetry and suggesting that in most cases flight performance is determined by the capability of the most damaged wing, not the average of all wings in these functionally two-winged insects. Thus, the cost of providing flight stability with asymmetric wings appears to be similar in magnitude to the benefit obtained from the additional area of the undamaged wing (Fernández et al., 2012).

This overall result is contrary to our initial hypothesis that insects might have evolved effective coping mechanisms for the stability problems of wing asymmetry or damage, as suggested by a number of studies finding little or no effect of wing damage on different aspects of flight performance. The opposing results of different studies of wing wear or damage may arise from different experimental protocols that produced qualitatively and quantitatively different amounts of damage. To examine this possibility, we divided our load-lifting data into large and small damage classes and found that for small amounts of damage (<12% of wing area), the effect of the damage was linearly proportional to the total loss of wing area with no additional penalty for wing asymmetry. This is consistent with prior results from *M. sexta* which showed that neuromuscular compensation for wing asymmetry begins once >10% of wing area is lost (Fernández et al., 2012), supporting a non-neural, biomechanical compensation mechanism in those cases where area loss is <10%.

### When is wing damage costly?

Different studies examining wing damage in insects have come to different conclusions as to the effect of wing damage on flight performance or costs. Results from artificial wing area reduction experiments in hawkmoths and dragonflies (Combes et al., 2010)

**Table 4. Respirometry and flight efficiency (lift to power ratio) for each experimental treatment**

| | Mass-specific $\dot{V}_{O_2}$ (ml g$^{-1}$ h$^{-1}$) | Mass-specific $\dot{V}_{CO_2}$ (ml g$^{-1}$ h$^{-1}$) | RQ | $P_{met}$ (W kg$^{-1}$) | $P_{mech}$ (W kg$^{-1}$) | Efficiency (N W$^{-1}$) |
|---|---|---|---|---|---|---|
| Unclipped | 51.60±2.08 | 41.36±2.32 | 0.80±0.03 | 288.25±11.90 | 54.72±0.81 | 19.18±0.97 |
| Asymmetric wings | 67.28±2.50 | 58.94±2.41 | 0.88±0.03 | 381.09±14.46 | 59.27±1.84 | 16.01±0.72 |
| Symmetric wings | 67.73±6.50 | 56.02±5.69 | 0.83±0.02 | 380.73±36.84 | 63.33±1.37 | 17.71±1.45 |

$\dot{V}_{O_2}$, oxygen consumption; $\dot{V}_{CO_2}$, carbon dioxide production; RQ, respiratory quotient; $P_{met}$, metabolic power; $P_{mech}$, estimated mechanical power. Values were generated using all individuals ($n$=6). Data are means±s.e.m. Data for each individual are available in Tables S1, S2 and S3.

Journal of Experimental Biology (2017) 220, 3649-3656 doi:10.1242/jeb.153494

**Table 5. Linear mixed-effects model showing the effect of treatment on metabolic power, predicted mechanical power, mass-specific $\dot{V}_{O_2}$, mass-specific $\dot{V}_{CO_2}$ and efficiency**

| Variable | *t*-value | *P*-value |
|---|---|---|
| $P_{met}$ | | |
| Unclipped vs asymmetric | 3.527 | 0.005 |
| Unclipped vs symmetric | 3.513 | 0.005 |
| Asymmetric vs symmetric | 0.013 | 0.989 |
| $P_{mech}$ | | |
| Unclipped vs asymmetric | 3.854 | 0.003 |
| Unclipped vs symmetric | 7.298 | <0.001 |
| Asymmetric vs symmetric | 3.443 | 0.006 |
| Mass-specific $\dot{V}_{O_2}$ | | |
| Unclipped vs asymmetric | 3.273 | 0.008 |
| Unclipped vs symmetric | 3.366 | 0.007 |
| Asymmetric vs symmetric | 0.093 | 0.928 |
| Mass-specific $\dot{V}_{CO_2}$ | | |
| Unclipped vs asymmetric | 5.093 | <0.001 |
| Unclipped vs symmetric | 4.245 | 0.002 |
| Asymmetric vs symmetric | 0.847 | 0.416 |
| Efficiency | | |
| Unclipped vs asymmetric | 2.737 | 0.021 |
| Unclipped vs symmetric | 1.233 | 0.245 |
| Asymmetric vs symmetric | 1.503 | 0.163 |
| RQ | | |
| Unclipped vs asymmetric | 2.704 | 0.022 |
| Unclipped vs symmetric | 0.851 | 0.414 |
| Asymmetric vs symmetric | 1.852 | 0.093 |

$P_{met}$, metabolic power; $P_{mech}$, estimated mechanical power; $\dot{V}_{O_2}$, mass-specific oxygen consumption; $\dot{V}_{CO_2}$, mass-specific carbon dioxide production; RQ, respiratory quotient.
Individual was used as a random effect.

demonstrated costs to wing area loss while artificial damage to bumblebees has revealed no metabolic cost (Hedenström et al., 2001) and only minimal flight biomechanics effects (Haas and Cartar, 2008). Damage to butterfly wings was not found to increase field mortality (Kingsolver, 1999), but the biomechanical consequences are unknown. The hawkmoth, dragonfly and bee studies (Combes et al., 2010; Hedenström et al., 2001) used similar methods, applied a qualitatively and quantitatively similar amount of damage and measured similar aspects of performance but reached opposing conclusions. This raises the possibility that differences in the flight physiology of the species in question account for the different results; moths and dragonflies use synchronous flight muscle while bumblebees use asynchronous muscle. Asynchronous flight muscle might facilitate biomechanical accommodation of wing damage by allowing for greater increases in flapping frequency in response to damage. Alternatively, maximum-effort experiments such as the asymptotic load-lifting tests may also more easily identify effects of wing damage on flight performance than the metabolic approach, which found no effect of wing damage in bumblebees (Hedenström et al., 2001). Such load-lifting tests have demonstrated that complete removal of the hindwing does reduce flight performance in bumblebees (Buchwald and Dudley, 2010). Similar results have been found for honey bees flying in hypodense gases, where reduced wing area and high asymmetry produced lower maximum wingtip velocities than obtained for bees with intact or symmetric wings, causing a greater impairment in maximal flight capacity (Vance and Roberts, 2014).

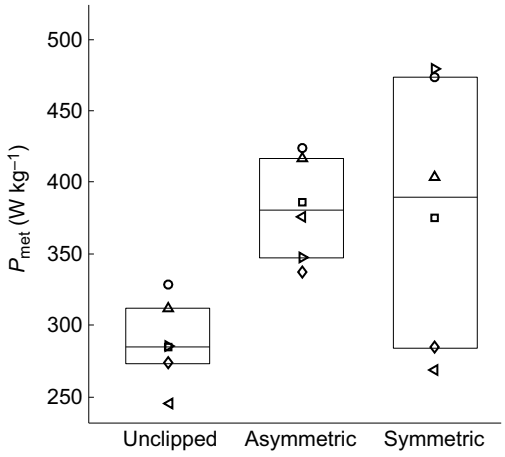


**Fig. 5. Effect of experimental treatment on metabolic power ($P_{met}$) measured by oxygen consumption and carbon dioxide production.** Boxes show the median, 25th and 75th percentile. Markers represent individual moths, but shape does not correspond to that in Figs 3 and 4 as the load-lifting experiments were conducted on a separate set of moths. Complete data on individual moths are provided in Tables S1–3; marker shape to moth ID is as follows: circles, moth 9; squares, moth 10; diamonds, moth 11; leftward triangle, moth 12; rightward triangle, moth 13; upward triangle, moth 14.

### Comparison with theoretical aerodynamic models

Our aerodynamic model of the effect of wing damage on maximum load-lifting capability predicted that the moths would increase flapping frequency or amplitude following wing clipping, allowing them to restore their aerodynamic power output to the level of an undamaged moth and making the reduction in load-lifting performance proportional to the cube root of the reduction in the second moment of area of the wings (Eqn 6). The underlying assumption of this model, that frequency or amplitude would change in response to clipping, was not supported, with only small and non-significant increases in frequency and amplitude observed. This result is in contrast to many other studies of wing damage in insects, including our prior result from hovering hawkmoths (Fernández et al., 2012). The difference in this experiment is that the flapping frequency of unclipped moths engaged in maximum load lifting was ∼30 Hz, already elevated above the ∼25 Hz commonly observed during hovering flight in this species. Wing clipping did not facilitate a further increase, suggesting that other factors such as minimum neuromuscular activation timing may ultimately limit flapping frequency in hawkmoths. This may not be the case for insects with asynchronous flight muscles. In keeping with the small and largely non-significant changes in flapping frequency and amplitude, the hawkmoth load-lifting results agree more closely with an aerodynamic model (Eqn 3) where flapping frequency and amplitude are constrained, which predicts a direct relationship between the proportional reduction in wing second moment of area and load-lifting capability. This suggests that the changes in frequency and amplitude, statistically significant or not, were insufficient to fully restore muscle power output to its original value or came at an additional cost to muscle contractile efficiency.

With regard to the metabolic power requirements of hovering flight, our results for moths following symmetric wing clipping were a close match to our simplest aerodynamic model (Eqn 7), where the change in the cost of hovering is proportional to the inverse square root of the change in the third moment of wing area. More complex modelling efforts such as re-solving Eqns 1 and 2 repeatedly for the different conditions in an attempt to include the interplay between the capacity for lift production and its cost were a poor fit to the data. These efforts predicted a much lower increase in hovering flight costs but also large increases in flapping frequency and thus might better fit results from insects with asynchronous flight muscles as bumblebees

were found to experience no detectable metabolic cost penalty from artificial wing area reduction (Hedenström et al., 2001).

The agreement between the metabolic data and our simplest aerodynamic model (Eqn 7) should not necessarily be taken as support for the mechanism – variation in flapping frequency only – used by the model. Many other changes in kinematic parameters such as variation in angle of attack or the timing of wing rotation could also increase the lift per unit area produced by a flapping wing and help compensate for wing area lost as a result of damage. However, as a general principle, increasing force per unit area decreases the lift to power ratio, so all these mechanisms would produce trends similar to those from Eqn 7.

## Conclusions

We found highly significant evidence of biomechanical performance consequences for wing wear or damage in hovering hawkmoths, in contrast to studies performed in bumblebees, where the consequences of damage to flight metabolism appear to be slight. We also found a significant cost of asymmetric damage for cases in which the damage exceeds ∼10% of wing area; smaller amounts of asymmetric damage produced no additional effect beyond total wing area loss. This varied response suggests that small asymmetries such as those typically implicated in fitness loss via sexual selection against fluctuating asymmetry (Watson and Thornhill, 1994) may have little to no functional consequence, even for structures as closely associated with flight costs as the wings of an insect. Natural losses in wing area such as those due to moulting in birds could also avoid any asymmetry penalty by remaining small.

## APPENDIX

The aerodynamic model used here includes the average square of non-dimensional angular velocity $\overline{(\mathrm{d}\hat{\phi}/\mathrm{d}\hat{t})^2}$ and the average absolute value of the cube of non-dimensional angular velocity $\overline{|\mathrm{d}\hat{\phi}/\mathrm{d}\hat{t}|^3}$. Numerical values of 19.74 and 105.29 are given, respectively, for these two quantities and noted in the text to represent sinusoidal motion. Non-dimensional angular velocity was described in Ellington (1984a), and represents normalization of angular motion to a range of −1 to 1, and time to a range of 0 to 1. Values of 19.74 and 105.29 were generated numerically in MATLAB by constructing a time sequence $t$ from 0 to 2π, calculating $\phi(t)=\sin(t)$, which is already limited to a range −1 to 1, so $\hat{\phi} = \phi$. Non-dimensional time is $\hat{t} = t/2\pi$ and from these values we numerically differentiated $\hat{\phi}$ and calculated the average of the squared or absolute value of the cubed derivative. These were 19.74 and 105.29 and thus represent the non-dimensional angular velocity for sinusoidal flapping.

### Acknowledgements

We wish to thank Dwight Springthorpe for assistance with the experiments.

### Competing interests

The authors declare no competing or financial interests.

### Author contributions

Conceptualization: T.L.H.; Methodology: M.J.F., M.E.D., T.L.H.; Formal analysis: M.J.F., T.L.H.; Investigation: M.J.F., M.E.D., T.L.H.; Resources: T.L.H.; Data curation: M.J.F., T.L.H.; Writing - original draft: M.J.F., T.L.H.; Writing - review & editing: M.J.F., T.L.H.; Supervision: T.L.H.; Project administration: T.L.H.; Funding acquisition: T.L.H.

### Funding

Funding was provided by the National Science Foundation (NSF IOS-0920358) to T.L.H.

### Supplementary information

Supplementary information available online at
http://jeb.biologists.org/lookup/doi/10.1242/jeb.153494.supplemental

### References

**Balmford, A., Jones, I. L. and Thomas, A. L. R.** (1993). On avian asymmetry: evidence of natural selection for symmetrical tails and wings in birds. *Proc. R. Soc. Lond. B Biol. Sci.* **252**, 245-251.

**Buchwald, R. and Dudley, R.** (2010). Limits to vertical force and power production in bumblebees (Hymenoptera: Bombus impatiens). *J. Exp. Biol.* **213**, 426-432.

**Cartar, R. V.** (1992). Morphological senescence and longevity: an experiment relating wing wear and life span in foraging wild bumble bees. *J. Anim. Ecol.* **61**, 225-231.

**Chai, P.** (1997). Hummingbird hovering energetics during moult of primary flight feathers. *J. Exp. Biol.* **200**, 1527-1536.

**Chai, P., Chen, J. S. C. and Dudley, R.** (1997). Transient hovering performance of hummingbirds under conditions of maximal loading. *J. Exp. Biol.* **200**, 921-929.

**Cheng, B., Tobalske, B. W., Powers, D. R., Hedrick, T. L., Wang, Y., Wethington, S. M., Chiu, G. T.-C. and Deng, X.** (2016). Flight mechanics and control of escape manoeuvres in hummingbirds. II. Aerodynamic force production, flight control and performance limitations. *J. Exp. Biol.* **219**, 3532-3543.

**Combes, S. A., Crall, J. D. and Mukherjee, S.** (2010). Dynamics of animal movement in an ecological context: dragonfly wing damage reduces flight performance and predation success. *Biol. Lett.* **6**, 426-429.

**Dickinson, M. H., Farley, C. T., Full, R. J., Koehl, M. A. R., Kram, R. and Lehman, S.** (2000). How animals move: an integrative view. *Science* **288**, 100-106.

**Dillon, M. E. and Dudley, R.** (2004). Allometry of maximum vertical force production during hovering flight of neotropical orchid bees (Apidae: Euglossini). *J. Exp. Biol.* **207**, 417-425.

**Ellington, C. P.** (1984a). The aerodynamics of hovering insect flight. III. Kinematics. *Philos. Trans. R. Soc. Lond. B Biol. Sci.* **305**, 41-78.

**Ellington, C. P.** (1984b). The aerodynamics of hovering insect flight. VI. Lift and power requirements. *Philos. Trans. R. Soc. Lond. B Biol. Sci.* **305**, 145-181.

**Fernández, M. J., Springthorpe, D. and Hedrick, T. L.** (2012). Neuromuscular and biomechanical compensation for wing asymmetry in insect hovering flight. *J. Exp. Biol.* **215**, 3631-3638.

**Haas, C. A. and Cartar, R. V.** (2008). Robust flight performance of bumble bees with artificially induced wing wear. *Can. J. Zool.* **86**, 668-675.

**Hambly, C., Harper, E. J. and Speakman, J. R.** (2004). The energetic cost of variations in wing span and wing asymmetry in the zebra finch *Taeniopygia guttata*. *J. Exp. Biol.* **207**, 3977-3984.

**Hedenström, A., Ellington, C. P. and Wolf, T. J.** (2001). Wing wear, aerodynamics and flight energetics in bumblebees (*Bombus terrestris*): an experimental study. *Funct. Ecol.* **15**, 417-422.

**Hedrick, T. L.** (2008). Software techniques for two- and three-dimensional kinematic measurements of biological and biomimetic systems. *Bioinspir. Biomim.* **3**, 034001.

**Hedrick, T. L., Cheng, B. and Deng, X.** (2009). Wingbeat time and the scaling of passive rotational damping in flapping flight. *Science* **324**, 252-255.

**Kingsolver, J. G.** (1999). Experimental analyses of wing size, flight, and survival in the western white butterfly. *Evolution* **53**, 1479-1490.

**Mountcastle, A. M., Alexander, T. M., Switzer, C. M. and Combes, S. A.** (2016). Wing wear reduces bumblebee flight performance in a dynamic obstacle course. *Biol. Lett.* **12**.

**Nishikawa, K., Biewener, A. A., Aerts, P., Ahn, A. N., Chiel, H. J., Daley, M. A., Daniel, T. L., Full, R. J., Hale, M. E., Hedrick, T. L. et al.** (2007). Neuromechanics: an integrative approach for understanding motor control. *Integr. Comp. Biol.* **47**, 16-54.

**Pinheiro, J. C. Bates, D. M.** (2000). *Mixed- Effects Models in S and S-Plus*. New York: Springer-Verlag.

**Ristroph, L., Bergou, A. J., Ristroph, G., Coumes, K., Berman, G. J., Guckenheimer, J., Wang, Z. J. and Cohen, I.** (2010). Discovering the flight autostabilizer of fruit flies by inducing aerial stumbles. *Proc. Natl. Acad. Sci. USA* **107**, 4820-4824.

**Springthorpe, D., Fernández, M. J. and Hedrick, T. L.** (2012). Neuromuscular control of free-flight yaw turns in the Hawkmoth *Manduca sexta*. *J. Exp. Biol.* **215**, 1766-1774.

**Swaddle, J. P.** (1997). Within-individual changes in developmental stability affect flight performance. *Behav. Ecol.* **8**, 601-604.

**Vance, J. T. and Roberts, S. P.** (2014). The effects of artificial wing wear on the flight capacity of the honey bee *Apis mellifera*. *J. Insect Physiol.* **65**, 27-36.

**Voigt, C. C.** (2013). Bat flight with bad wings: is flight metabolism affected by damaged wings? *J. Exp. Biol.* **216**, 1516-1521.

**Watson, P. J. and Thornhill, R.** (1994). Fluctuating asymmetry and sexual selection. *Trends Ecol. Evol.* **9**, 21-25.

**Weis-Fogh, T.** (1973). Quick estimates of flight fitness in hovering animals, including novel mechanisms for lift production. *J. Exp. Biol.* **59**, 169-230.

**Zheng, L., Hedrick, T. L. and Mittal, R.** (2013). A multi-fidelity modelling approach for evaluation and optimization of wing stroke aerodynamics in flapping flight. *J. Fluid Mech.* **721**, 118-154.



Journal of Experimental Biology

Supplementary Data

Table S1. Morphological parameters for each individual during control (full wings) and clipped wing treatments. Moths 1- 8 were used for the load-lifting experiment and moths 9 – 15 were used for the respirometry experiment. Asymmetric trials were recorded from moths 1, 2, 10, 11, 12, 13, 14 after clipping the right wing (R) and in moths 3, 4, 5, 6, 7, 8, 9 after clipping the left wing (L).

| Moth | Treatment | Wing area ($cm^2$) | | Length (cm) | | $2^{nd}$ moment ($cm^4$) | | $3^{rd}$ moment ($cm^5$) | | Total Clip (%) | |
|---|---|---|---|---|---|---|---|---|---|---|---|
| | | L | R | L | R | L | R | L | R | L | R |
| 1 | Control | 7.42 | 7.53 | 5.34 | 5.31 | 73.53 | 76.94 | 280.24 | 295.38 | 10.17 | 9.35 |
| | Clipped | 6.67 | 6.83 | 4.52 | 4.54 | 54.78 | 59.58 | 188.12 | 210.07 | | |
| 2 | Control | 7.28 | 7.14 | 5.13 | 5.19 | 64.66 | 65.57 | 233.63 | 239.49 | 9.40 | 8.68 |
| | Clipped | 6.59 | 6.52 | 4.41 | 4.38 | 50.42 | 50.39 | 167.44 | 167.80 | | |
| 3 | Control | 6.86 | 6.91 | 5.27 | 5.28 | 65.95 | 66.60 | 244.82 | 247.67 | 22.86 | 18.46 |
| | Clipped | 5.29 | 5.63 | 3.80 | 4.00 | 33.42 | 39.70 | 99.33 | 124.85 | | |
| 4 | Control | 6.53 | 6.62 | 4.94 | 4.95 | 57.02 | 56.42 | 202.11 | 197.81 | 14.23 | 16.28 |
| | Clipped | 5.60 | 5.54 | 4.07 | 3.90 | 39.25 | 36.65 | 123.12 | 111.87 | | |
| 5 | Control | 6.03 | 6.15 | 4.57 | 4.70 | 44.83 | 46.26 | 147.67 | 153.86 | 16.16 | 21.97 |
| | Clipped | 5.06 | 4.80 | 3.71 | 3.49 | 28.26 | 25.04 | 79.89 | 68.20 | | |
| 6 | Control | 6.67 | 6.43 | 5.19 | 4.93 | 59.18 | 52.44 | 215.17 | 181.78 | 12.06 | 11.75 |
| | Clipped | 5.87 | 5.67 | 4.24 | 4.18 | 42.34 | 38.46 | 136.68 | 120.54 | | |
| 7 | Control | 7.27 | 7.27 | 5.06 | 4.94 | 62.18 | 65.65 | 222.19 | 238.13 | 9.18 | 8.37 |
| | Clipped | 6.61 | 6.67 | 4.60 | 4.46 | 51.13 | 53.91 | 171.19 | 183.72 | | |
| 8 | Control | 7.29 | 7.23 | 5.37 | 5.16 | 74.04 | 65.67 | 282.34 | 239.66 | 7.52 | 8.43 |
| | Clipped | 6.75 | 6.62 | 4.77 | 4.42 | 61.44 | 52.69 | 220.01 | 177.74 | | |
| 9 | Control | 8.92 | 9.66 | 4.35 | 4.68 | 49.34 | 61.18 | 152.61 | 202.78 | 23.22 | 24.57 |
| | Clipped | 6.85 | 7.28 | 3.46 | 3.78 | 21.94 | 33.50 | 51.22 | 92.51 | | |
| 10 | Control | 9.41 | 9.18 | 5.32 | 4.94 | 70.33 | 62.57 | 250.10 | 209.11 | 10.01 | 9.26 |
| | Clipped | 8.47 | 8.32 | 4.24 | 3.92 | 48.16 | 45.81 | 147.89 | 137.48 | | |
| 11 | Control | 11.01 | 10.54 | 5.46 | 5.60 | 85.54 | 84.18 | 309.88 | 317.97 | 11.33 | 12.17 |
| | Clipped | 9.76 | 9.25 | 4.10 | 4.10 | 53.22 | 49.06 | 159.82 | 147.56 | | |
| 12 | Control | 10.62 | 10.54 | 5.34 | 5.60 | 76.63 | 84.88 | 267.95 | 317.97 | 7.62 | 9.70 |
| | Clipped | 9.81 | 9.52 | 4.41 | 4.39 | 57.57 | 56.10 | 180.66 | 178.43 | | |
| 13 | Control | 9.63 | 9.32 | 5.25 | 5.17 | 70.47 | 66.61 | 247.77 | 230.41 | 9.90 | 9.91 |
| | Clipped | 8.68 | 8.40 | 4.15 | 4.13 | 49.78 | 47.27 | 152.72 | 142.26 | | |
| 14 | Control | 9.13 | 8.77 | 4.99 | 4.83 | 58.59 | 51.68 | 195.24 | 167.07 | 8.40 | 8.24 |
| | Clipped | 8.36 | 8.05 | 4.13 | 3.89 | 46.81 | 38.17 | 140.53 | 109.89 | | |

Table S2. Maximum load and wing kinematics data

| Moth | Treatment | Mass (g) | Max. Force (mN) | Flapping Frequency (Hz) | Flapping Amplitude R – (Deg.) | Flapping amplitude L – (Deg.) |
|---|---|---|---|---|---|---|
| 1 | Control | 1.76 | 29.11 | 28.74 | 114.7 | 117.6 |
| | Asymmetric | 1.69 | 24.53 | 28.07 | 110.4 | 110.7 |
| | Symmetric | 1.45 | 24.16 | 29.01 | 115.6 | 113.2 |
| 2 | Control | 1.49 | 26.53 | 27.34 | 122.0 | 121.8 |
| | Asymmetric | 1.54 | 25.01 | 28.87 | 123.7 | 116.0 |
| | Symmetric | 1.48 | 22.48 | 29.27 | 117.5 | 129.9 |
| 3 | Control | 1.46 | 26.05 | 31.05 | 109.3 | 106.9 |
| | Asymmetric | 1.38 | 17.48 | 32.27 | 87.4 | 134.0 |
| | Symmetric | 1.35 | 16.22 | 30.32 | 122.9 | 131.8 |
| 4 | Control | 1.41 | 21.75 | 27.26 | 115.9 | 106.9 |
| | Asymmetric | 1.27 | 16.49 | 29.31 | 108.0 | 128.8 |
| | Symmetric | 1.24 | 16.15 | 29.25 | 119.8 | 127.2 |
| 5 | Control | 1.44 | 22.00 | 29.49 | 130.1 | 117.0 |
| | Asymmetric | 1.21 | 15.82 | 29.52 | 107.4 | 124.0 |
| | Symmetric | 1.24 | 14.07 | 29.97 | 123.0 | 119.9 |
| 6 | Control | 1.54 | 27.31 | 29.03 | 120.5 | 115.7 |
| | Asymmetric | 1.49 | 19.03 | 29.27 | 106.8 | 121.9 |
| | Symmetric | 1.42 | 20.09 | 30.01 | 120.6 | 121.2 |
| 7 | Control | 1.57 | 24.23 | 28.55 | 125.6 | 113.8 |
| | Asymmetric | 1.86 | 26.20 | 28.38 | 121.6 | 121.5 |
| | Symmetric | 1.66 | 24.27 | 30.06 | 120.0 | 125.2 |
| 8 | Control | 1.58 | 27.76 | 27.01 | 125.5 | 127.9 |
| | Asymmetric | 1.53 | 24.93 | - | - | - |
| | Symmetric | 1.50 | 25.10 | 28.10 | 131.6 | 126.9 |

Table S3. Oxygen consumption and carbon dioxide production data

| Moth | Treatment | Mass (g) | $\dot{V}O_2$ (ml hr$^{-1}$) | VCO2 (ml hr$^{-1}$) |
|---|---|---|---|---|
| 9 | Control | 1.56 | 90.80 | 77.07 |
| | Asymmetric | 1.56 | 115.76 | 102.03 |
| | Symmetric | 1.57 | 134.48 | 103.70 |
| 10 | Control | 1.67 | 88.04 | 59.78 |
| | Asymmetric | 1.63 | 112.14 | 92.56 |
| | Symmetric | 1.63 | 108.12 | 92.38 |
| 11 | Control | 1.73 | 84.34 | 68.8 |
| | Asymmetric | 1.63 | 96.79 | 82.84 |
| | Symmetric | 1.53 | 77.30 | 64.12 |
| 12 | Control | 1.89 | 83.56 | 65.49 |
| | Asymmetric | 1.63 | 109.65 | 87.29 |
| | Symmetric | 1.62 | 78.15 | 61.08 |
| 13 | Control | 1.69 | 84.06 | 75.57 |
| | Asymmetric | 1.61 | 96.78 | 99.26 |
| | Symmetric | 1.50 | 126.17 | 111.23 |
| 14 | Control | 1.29 | 72.32 | 56.63 |
| | Asymmetric | 1.23 | 89.64 | 79.37 |
| | Symmetric | 1.12 | 80.25 | 67.10 |